Supporting Information

Giant thermal expansion associated with macroscopic polarization change in a single crystal of Zn(II) complex

Zheng Tang,[a] Chengdong Liu,[a] Yan Zhang,[a] Xiao-Peng Sun,[b] Jun Tao*[a], and Zi-Shuo Yao,*[a]

[a]Key Laboratory of Cluster Science of Ministry of Education, School of Chemistry and Chemical Engineering, Liangxiang Campus, Beijing Institute of Technology, Beijing 102488, People's Republic of China

[b]Henan Key Laboratory of Polyoxometalate Chemistry, College of Chemistry and Chemical Engineering, Henan University, Kaifeng 475004, People's Republic of China

*E-mail: zishuoyao@bit.edu.cn; taojun@bit.edu.cn.

Contents

EXPERIMENTAL **SEC**TION

Measurements. The elemental analyses of C, H, and N for compound **1** were collected on EUROVECTER EA3000 analyzer (Italy). Differential scanning calorimetry (DSC) were measured on PerkinElmer DSC 8000 with a scan rate of 10 K min^{-1}. The pictures of crystal sample used in the pyroelectric test were recorded on a stereo microscope MZ61. Pyroelectric measurements were conducted on Keithley 6517B electrometer equipped with Quantum Design MPMS XL7 temperature controller, using helium gas flow to restrict the temperature between 90 and 220 K with the scan rate of 2 K min^{-1}. The crystal (001) and (00–1) faces of a single-crystal sample (0.09 × 0.09 × 0.94 mm^3) were fixed with Conductive Silver Glue.

Theoretical calculations

The dipolar moments of **1** at different temperatures were performed with Gaussian 09 software package using the B3LYP/6–311G* level[1]. The program *PASCal* was employed to calculate the thermal expansion coefficients for different crystallographic axes[2].

Table S1. Crystallographic parameters for 1 at different temperatures.

[Zn(4-ethylpyridine)$_2$(NCS)$_2$] (1)							
Formula	$ZnC_{16}N_4S_2H_{18}$						
M / gmol^{-1}	395.83						
T / K	90(2)	107(2)	150(2)	210(2)	260(2)	293(2)	340(2)
Crystal system	Orthorhombic						
Space group	*Fdd*2						
a / Å	19.4675(8)	19.4649(12)	19.3601(17)	19.2930(3)	19.2330(3)	19.2312(17)	19.1290(2)
b / Å	39.9414(14)	39.9750(3)	39.9640(3)	39.9040(4)	39.8240(4)	39.7900(3)	39.5670(5)
c / Å	4.8733(2)	4.9043(3)	4.9941(5)	5.0950(5)	5.1898(7)	5.2604(4)	5.3374(5)
α / °	90	90	90	90	90	90	90
β / °	90	90	90	90	90	90	90
γ / °	90	90	90	90	90	90	90
V / Å^3	3789.3(3)	3816.1(5)	3864.0(6)	3922.5(8)	3975.0(8)	4025.3(5)	4039.7(7)
Z	8	8	8	8	8	8	8
D_c / g cm^{-3}	1.388	1.378	1.361	1.341	1.323	1.306	1.302
μ / mm^{-1}	1.520	1.509	1.490	1.468	1.449	1.430	1.425
F(000)	1632.0	1632.0	1632.0	1632.0	1632.0	1632.0	1632.0
*R*int	0.0924	0.0569	0.0261	0.0220	0.0239	0.0221	0.0412
Completeness	0.998	0.997	0.997	0.999	0.994	0.992	0.994
R_1 [$I \geq 2\sigma(I)$][a]	0.0968	0.0761	0.0373	0.0410	0.0400	0.0393	0.0393
wR_2 [all data][b]	0.2285	0.1686	0.0967	0.1144	0.1291	0.1350	0.1179
GOF	1.136	1.139	1.066	1.036	1.028	1.030	0.915
max, min Δρ, e Å^{-3}	0.941/-0.668	0.555/-0.695	0.328/-0.247	0.298/-0.207	0.277/-0.190	0.246/-0.171	0.130/-0.144
CCDC	2214726	2214727	2214728	2214729	2214730	2214731	2214732

[a] $R_1 = \sum||F_o| - |F_c||/\sum|F_o|$, [b] $wR_2 = [\sum w(F_o^2 - F_c^2)^2/\sum w(F_o^2)^2]^{1/2}$

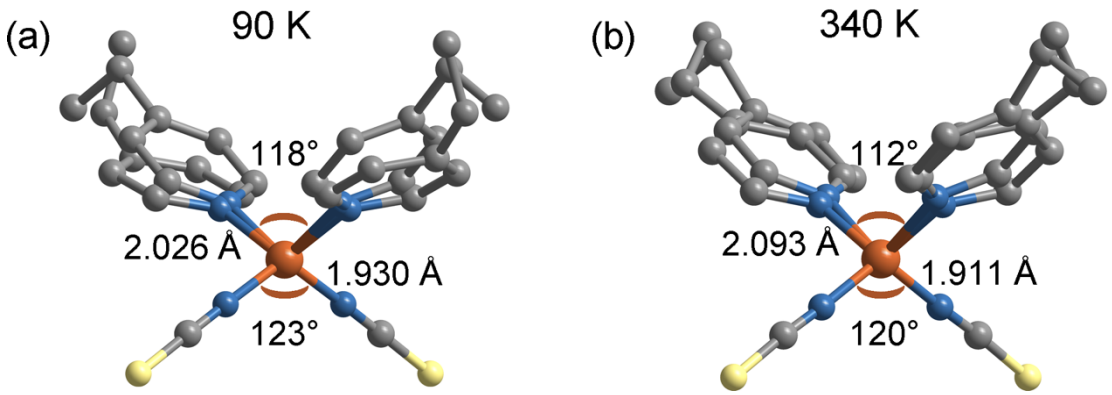

Figure S1. Molecular structures of compound **1** at 90 K and 340 K.

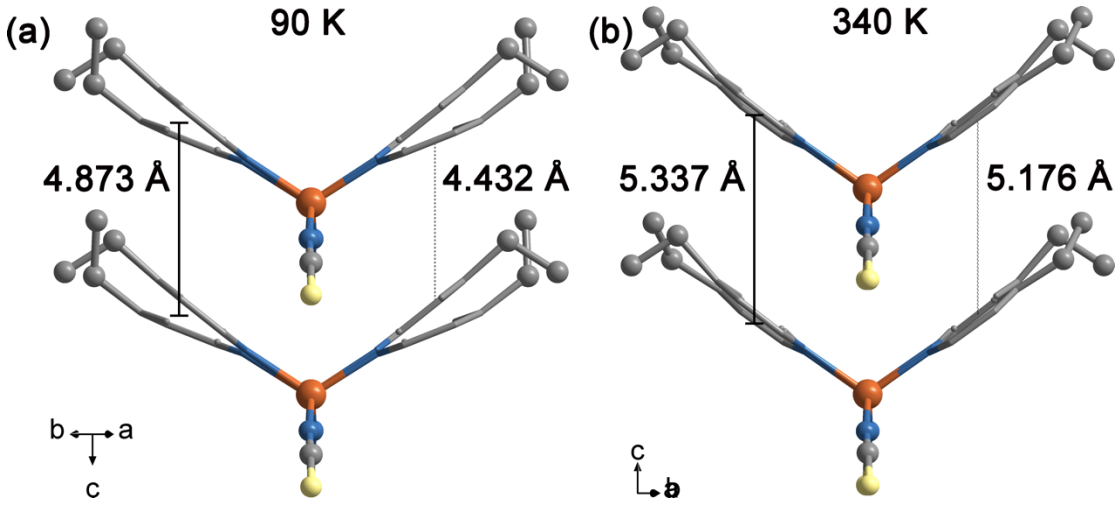

Figure S2. The intermolecular interactions in the 1D molecular column of compound **1** at 90 and 340 K.

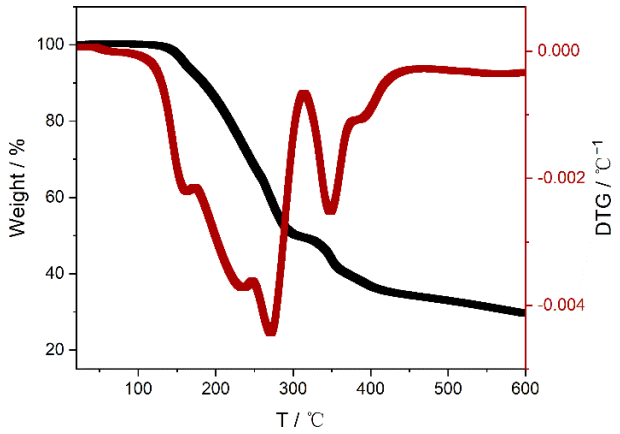

Figure S3. TG and DTG curves of compound **1.**

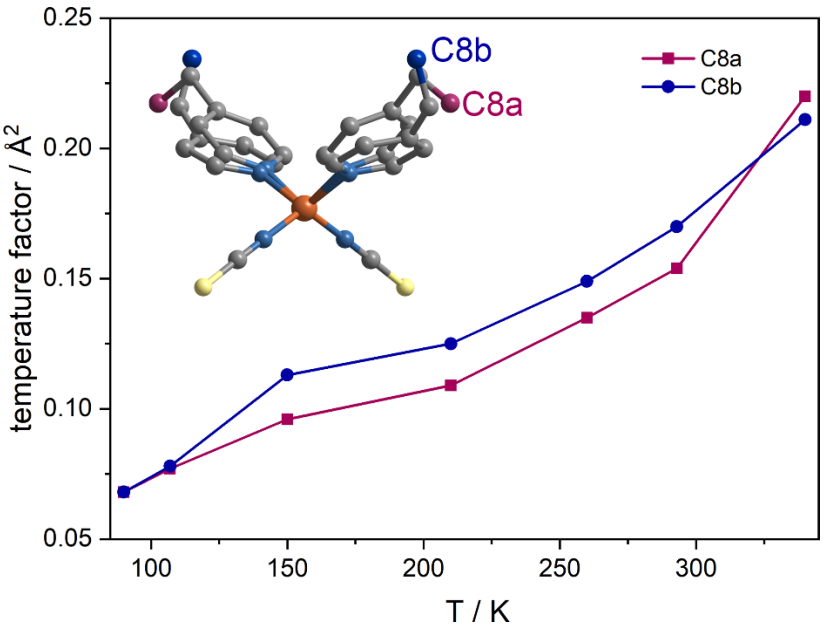

Figure S4. The temperature factors of C8 (carbon atoms on substituent group) at different temperatures.

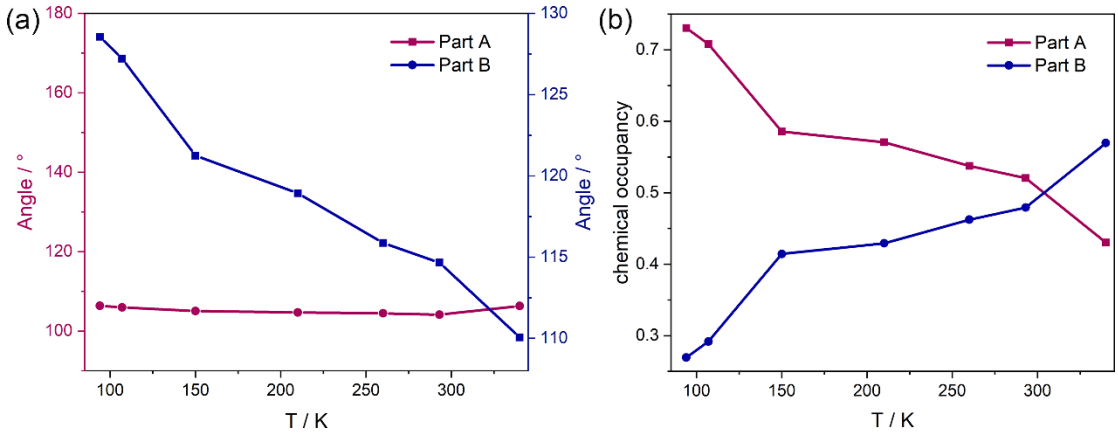

Figure S5. The variation of the occupation ratio and corresponding dihedral angle of disorder structure upon heating.

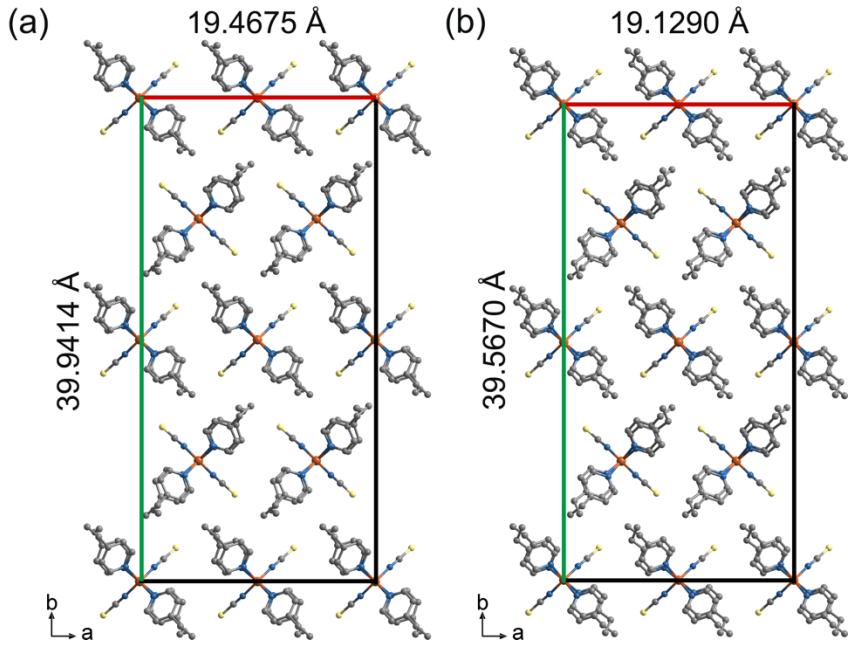

Figure S6. The packing structure of compound **1** at 90 K (a) and 340 K (b).

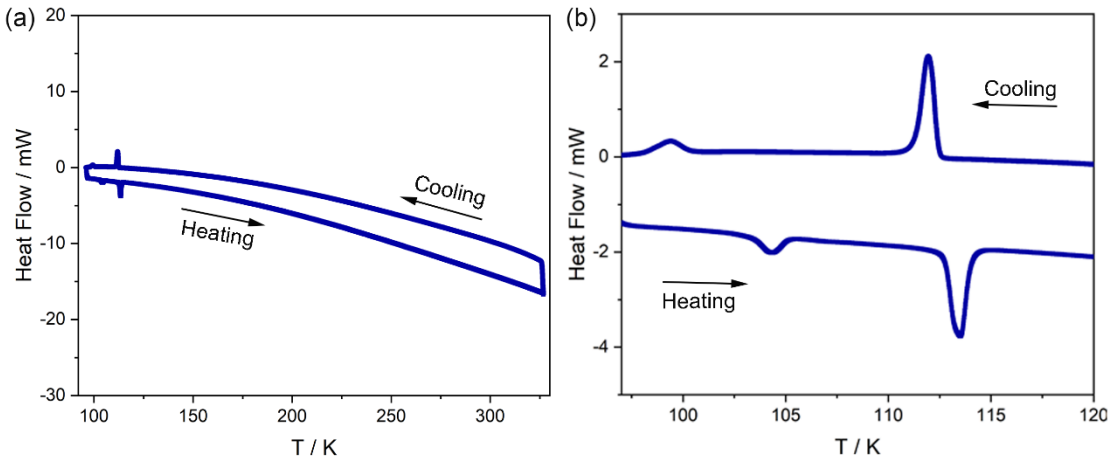

Figure S7. DSC curves of compound **1** (scan rate: 10 K min^{-1}).

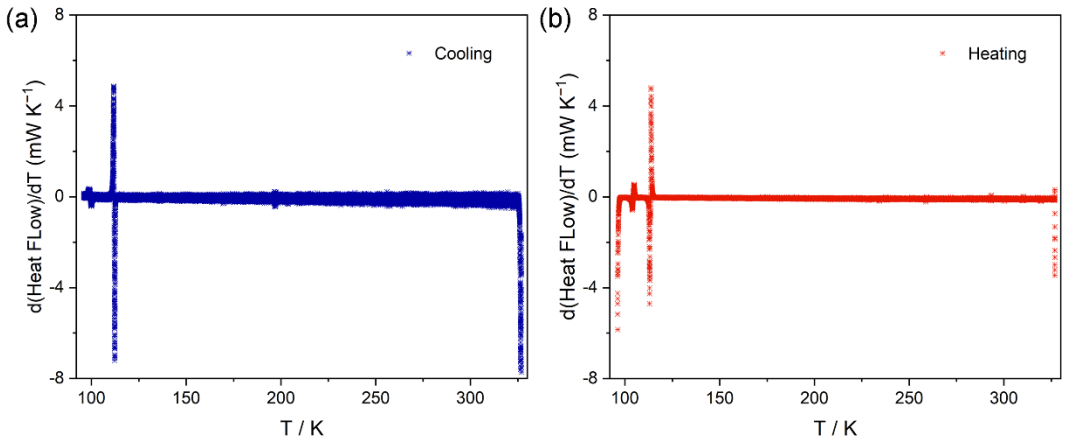

Figure S8. The first-order derivative of the heat flow of compound **1** during the DSC cooling (a) and heating (b) process. The phase transition can only be detected in the temperature range of 90–120 K.

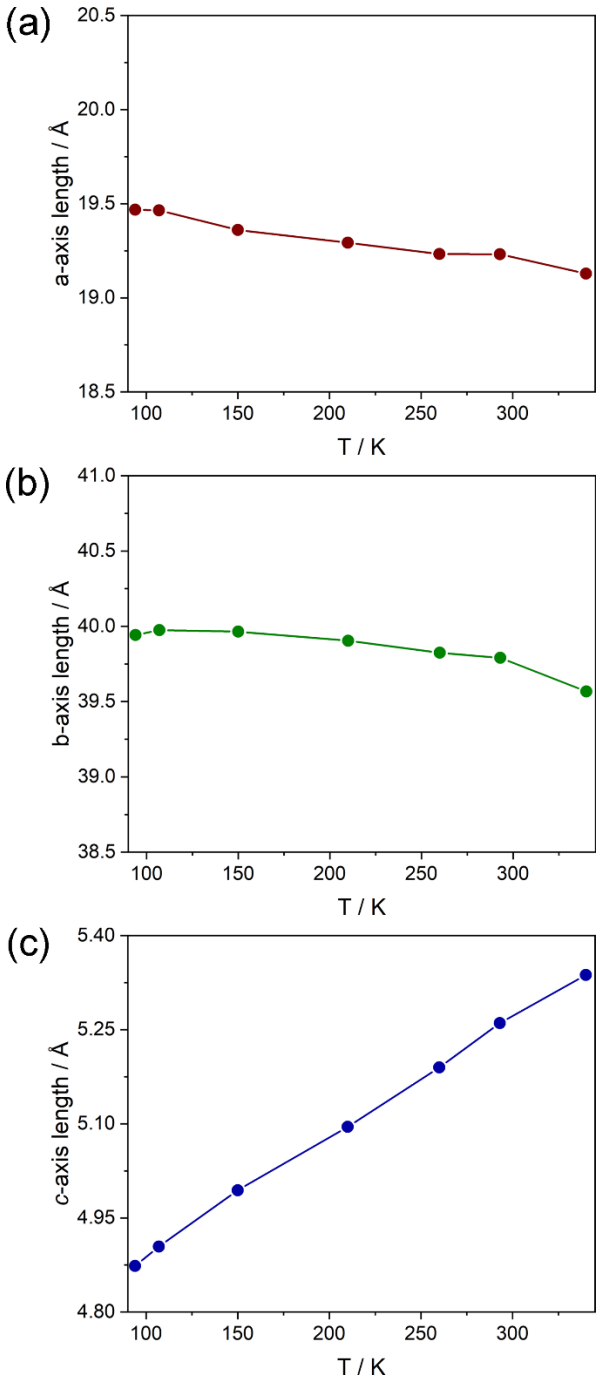

Figure S9. Temperature-dependent cell parameters of compound **1** in the temperature range of 90–340 K**.** (a) Variation in the *a*-axis length. (b) Variation in the *b*-axis length. (c) Variation in the *c*-axis length. The cell lengths of the *a*- and *b*- axes slightly decreases while the cell length of *c*- axes rapidly increases.

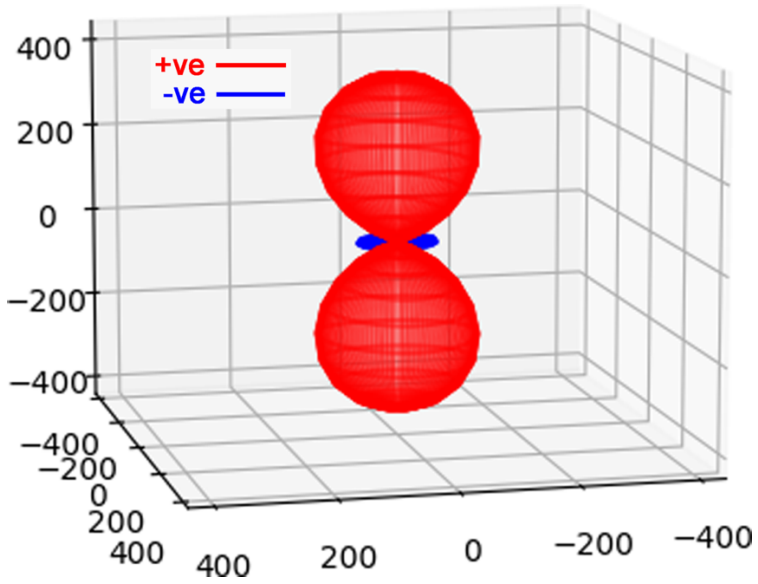

Figure S10. *PASCal* [2] expansivity indicatrices for compound **1**.

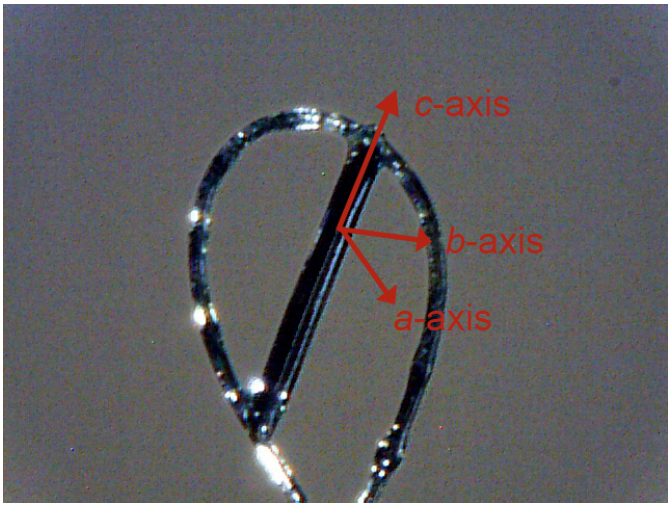

Figure S11. Face index of compound **1.**

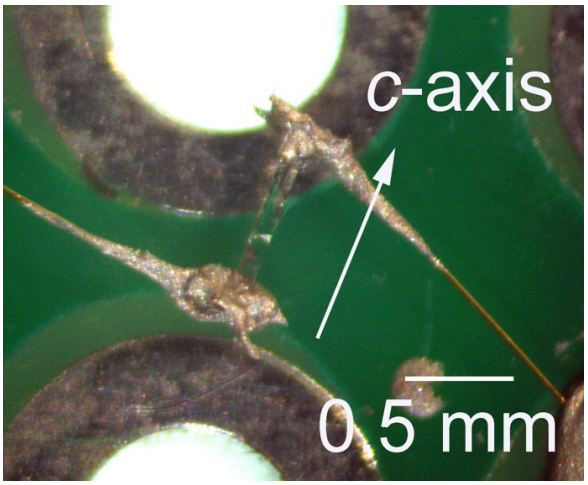

Figure S12. The photograph of single-crystal sample **1** in the pyroelectric measurement.

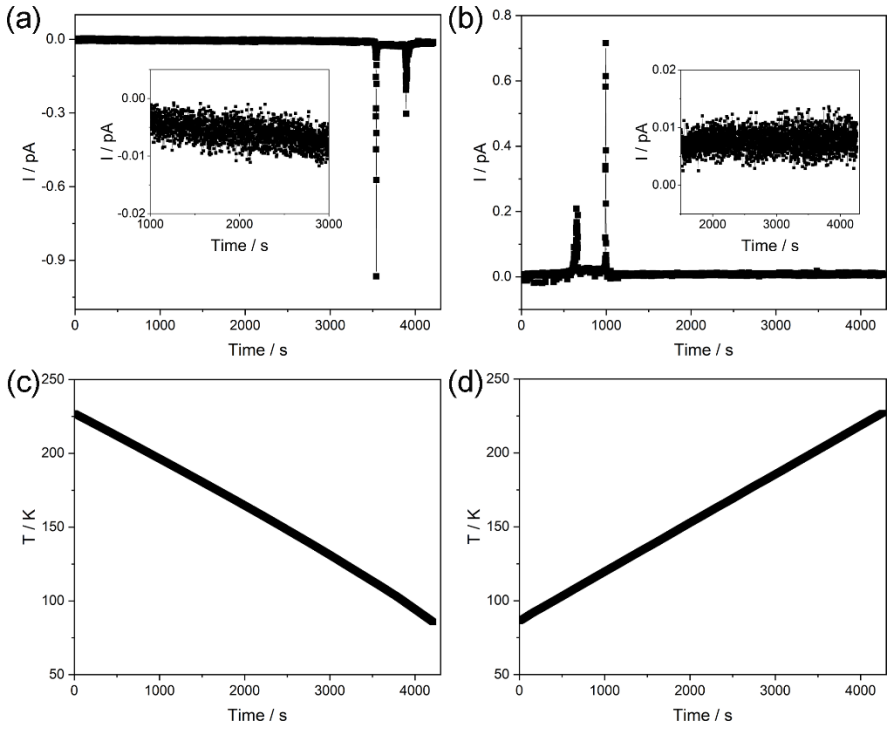

Figure S13. Summary of original data of compound **1** in pyroelectric coefficient test.

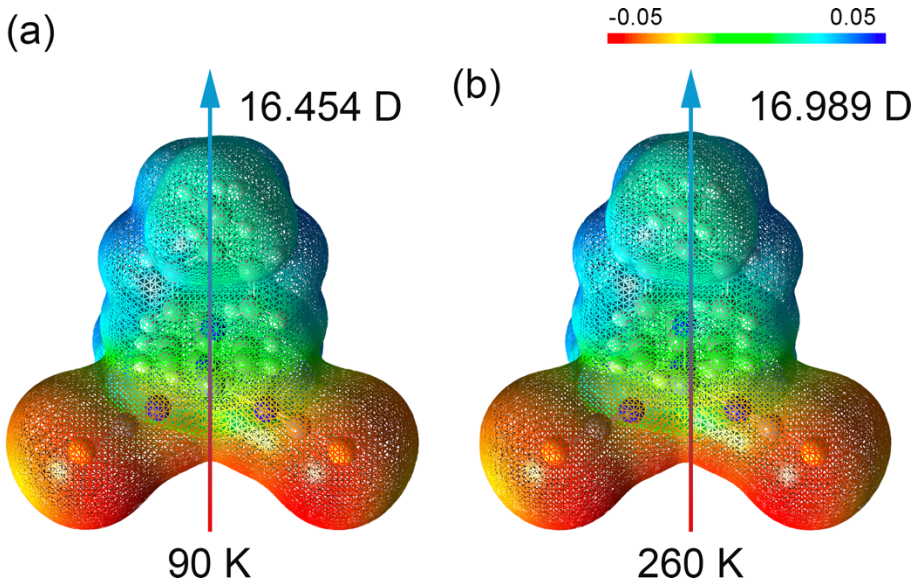

Figure S14. The dipole moment of partial structure (part A) in compound **1**, in which the red area represents the negative charge and the blue area represents the positive charge.

Table S2. Crystallographic parameters for **2** and **3** at different temperatures.

	[Zn(4-isopropylpyridine)$_2$(NCS)$_2$] (**2**)		[Zn(4-tert-butylpyridine)$_2$(NCS)$_2$] (**3**)	
Formula	$ZnC_{18}N_4S_2H_{22}$		$ZnC_{20}N_4S_2H_{26}$	
M / gmol^{-1}	423.93		451.99	
T / K	120	340	120	340
Crystal system	Orthorhombic			
Space group	*Fdd*2			
a / Å	19.6144(14)	19.8909(9)	20.2823(7)	20.9648(8)
b / Å	37.3980(6)	38.0008(15)	39.1046(17)	38.3960(15)
c / Å	5.6808(5)	5.8551(3)	5.8157(2)	5.9561(2)
α / °	90	90	90	90
β / °	90	90	90	90
γ / °	90	90	90	90
V / Å^3	4167.1(8)	4425.7(3)	4612.6(3)	4794.4(3)
Z	8	8	8	8
D_c / g cm^{-3}	1.351	1.272	1.302	1.252
μ / mm^{-1}	1.387	1.306	1.257	1.210
F(000)	1760.0	1760.0	1888.0	1888.0
Rint	0.0874	0.0270	0.0319	0.0300
Completeness	0.995	0.995	0.971	0.997
R_1 [$I \geq 2\sigma(I)$][a]	0.0890	0.0410	0.0221	0.0318
wR_2 [all data][b]	0.2562	0.1377	0.0559	0.0959
GOF	1.102	1.023	1.062	1.035
max, min Δρ, e Å^{-3}	0.803/-1.630	0.209/-0.192	0.236/-0.166	0.207/-0.195
CCDC	2216171	2216172	2216173	2216174

[a]$R_1 = \sum||F_o| - |F_c||/\sum|F_o|$, [b]$wR_2 = [\sum w(F_o^2 - F_c^2)^2/\sum w(F_o^2)^2]^{1/2}$

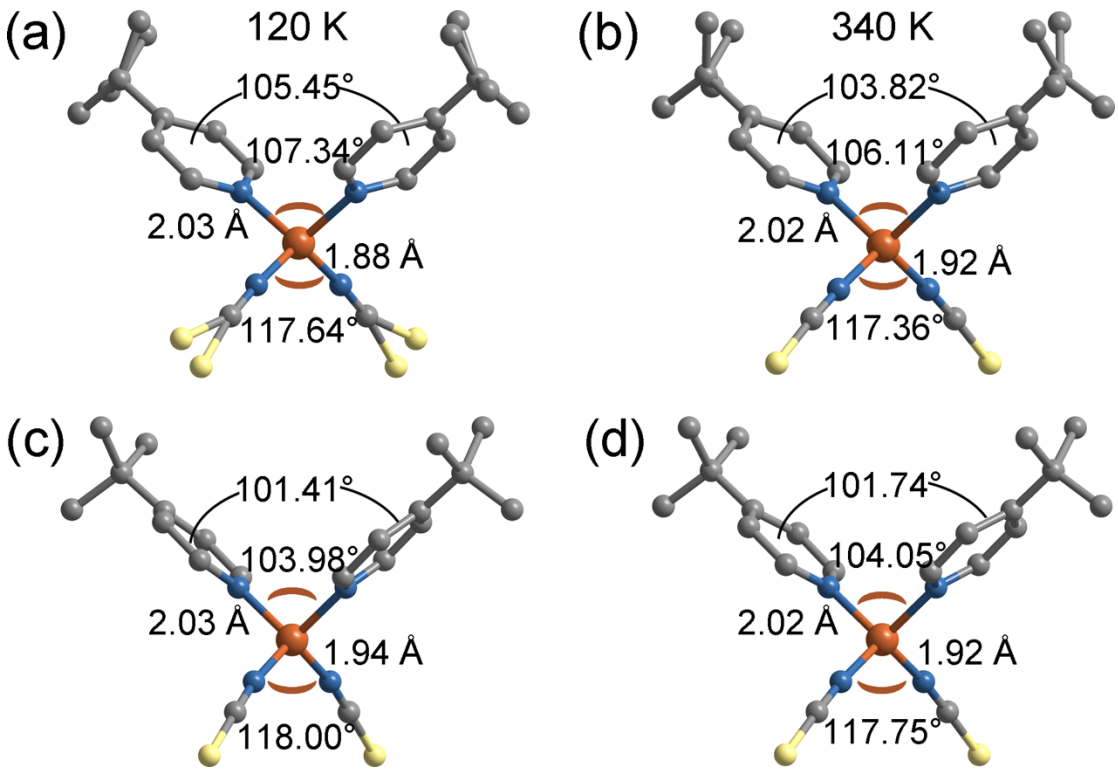

Figure S15. The molecular structures of compounds [Zn(4-isopropylpyridine)$_2$(NCS)$_2$] (a, b), and [Zn(4-tert-butylpyridine)$_2$(NCS)$_2$] (c, d) at 120 and 340 K.

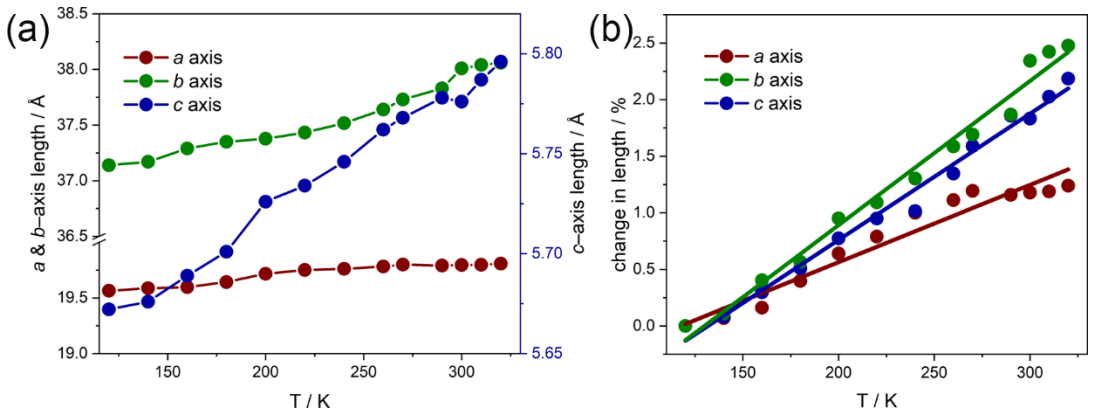

Figure S16. Thermal expansion behaviour of compound **2**. (a) Temperature dependence cell parameters. (b) Linear thermal expansion coefficients calculated from *PASCal*.

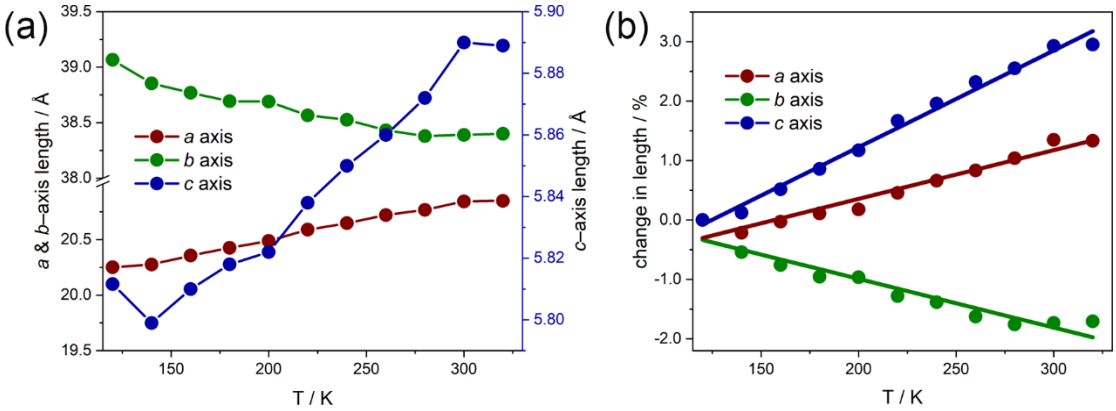

Figure S17. Thermal expansion behaviour of compound **3**. (a) Temperature dependence cell parameters. (b) Linear thermal expansion coefficients calculated from *PASCal*.

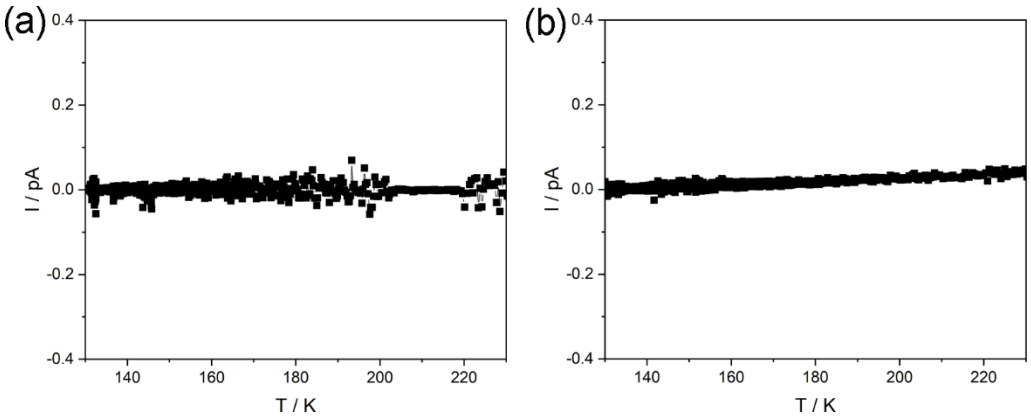

Figure S18. Pyroelectric current of compounds **2** (a), and **3** (b).

Reference

1. Frisch, M.; Trucks, G.; Schlegel, H.; Scuseria, G.; Robb, M.; Cheeseman, J.; Scalmani, G.; Barone, V.; Mennucci, B.; Petersson, G. Gaussian 09; Gaussian, Inc. *Wallingford, CT.* **2009,** *32*, 5648-5652.

2. Cliffe, M. J.; Goodwin, A. L. PASCal: a principal axis strain calculator for thermal expansion and compressibility determination. *Journal of Applied Crystallography.* **2012,** *45*, 1321-1329.